Cell Death and Differentiation (2013) 20, 920–930

www.nature.com/cdd

PINK1 protects against cell death induced by mitochondrial depolarization, by phosphorylating Bcl-xL and impairing its pro-apoptotic cleavage

G Arena[1,2], V Gelmetti[1], L Torosantucci[1], D Vignone[1], G Lamorte[1], P De Rosa[1,2], E Cilia[1], EA Jonas[3] and EM Valente*[,1,4]

Mutations in the *PINK1* gene are a frequent cause of autosomal recessive Parkinson's disease (PD). *PINK1* encodes a mitochondrial kinase with neuroprotective activity, implicated in maintaining mitochondrial homeostasis and function. In concurrence with Parkin, PINK1 regulates mitochondrial trafficking and degradation of damaged mitochondria through mitophagy. Moreover, PINK1 can activate autophagy by interacting with the pro-autophagic protein Beclin-1. Here, we report that, upon mitochondrial depolarization, PINK1 interacts with and phosphorylates Bcl-xL, an anti-apoptotic protein also known to inhibit autophagy through its binding to Beclin-1. PINK1–Bcl-xL interaction does not interfere either with Beclin-1 release from Bcl-xL or the mitophagy pathway; rather it protects against cell death by hindering the pro-apoptotic cleavage of Bcl-xL. Our data provide a functional link between PINK1, Bcl-xL and apoptosis, suggesting a novel mechanism through which PINK1 regulates cell survival. This pathway could be relevant for the pathogenesis of PD as well as other diseases including cancer.
Cell Death and Differentiation (2013) **20,** 920–930; doi:10.1038/cdd.2013.19; published online 22 March 2013

Parkinson's disease (PD) is the second most common neurodegenerative disorder after Alzheimer's disease, with prevalence of 1% in the population older than 60 years.[1] Several biochemical abnormalities, including mitochondrial dysfunction, oxidative stress and misfolded protein damage, have been implicated in PD pathogenesis.[2] Although the majority of late-onset cases are sporadic, early-onset PD is frequently caused by mutations in genes with autosomal recessive inheritance, mainly *Parkin* (GeneID: 5071) and *PINK1* (GeneID: 65018).[3]

PINK1 encodes a 63 kDa mitochondrial protein kinase, which is processed by mitochondrial proteases to generate two smaller isoforms.[4–7] We and others have shown that PINK1 acts as a key neuroprotective protein, aimed at preventing mitochondrial dysfunction and apoptotic cell death in response to multiple stress conditions.[8–10] This pro-survival activity is exerted through several mechanisms, including phosphorylation of the mitochondrial proteins TRAP1 and Omi/HtrA2, and regulation of mitochondrial calcium buffering.[11–14]

Increasing data now indicate that PINK1 acts upstream of Parkin in an evolutionary conserved pathway implicated in regulating mitochondrial biogenesis, trafficking and fusion/fission events, to maintain mitochondrial network health.[15] In particular, upon mitochondrial depolarization, PINK1 processing is impaired, determining a marked accumulation of the full-length protein on the surface of dysfunctional mitochondria, where it recruits Parkin. This process results in the phosphorylation and/or ubiquitination of several mitochondrial substrates, leading to the selective quarantine of damaged mitochondria and their degradation through mitophagy.[16–19] In line with this, we reported that coexpression of mutant, but not wild-type (wt) PINK1, with mutant alpha-synuclein resulted in the formation of enlarged autophagosomes surrounding abnormal mitochondria, as well as accumulation of degenerated mitochondria within autophagosomes.[12] Moreover, we recently demonstrated that PINK1 is able to activate basal and starvation-induced autophagy through its interaction with Beclin-1, a main pro-autophagic protein already implicated in the pathogenesis of other neurodegenerative diseases.[20]

Herein, we show that PINK1 interacts with, and phosphorylates Bcl-xL, a key anti-apoptotic protein of the Bcl-2 family also known to regulate Beclin-1 mediated autophagy. Our results indicate that, upon mitochondrial depolarization, PINK1-dependent Bcl-xL phosphorylation is not involved in autophagy/mitophagy activation, but significantly protects against apoptotic cell death.

Results

PINK1 interacts with Bcl-xL on depolarized mitochondria. As PINK1 binds to Beclin-1, we hypothesized that it could regulate autophagy by interacting with specific members of the Beclin-1 core complex involved in autophagosome formation.[21] In particular, we focused on the anti-apoptotic protein Bcl-xL, which is highly expressed at

[1]Neurogenetics Unit, Mendel Laboratory, IRCCS Casa Sollievo della Sofferenza, San Giovanni Rotondo, FG, Italy; [2]Department of Molecular Medicine, Sapienza University, Rome, Italy; [3]Department of Internal Medicine, Yale University, New Haven, CT, USA and [4]Department of Medicine and Surgery, University of Salerno, Salerno, Italy
*Corresponding author: EM Valente, Neurogenetics Unit, Mendel Laboratory, IRCCS Casa Sollievo della Sofferenza, Viale Regina Margherita 261, Rome 00198, Italy. Tel: +39 06 44160537; Fax: +39 06 44160548; E-mail: e.valente@css-mendel.it
Keywords: apoptosis; mitochondria; Parkinson's disease; post-translational modifications.
Received 20.8.12; revised 01.2.13; accepted 09.2.13; Edited by JM Hardwick; published online 22.3.13

neuronal level and is known to inhibit autophagy through its interaction with Beclin-1.[22,23] In line with this hypothesis, we demonstrated that overexpressed PINK1 and Bcl-xL strongly interacted in HEK293 cells subjected to reciprocal co-immunoprecipitation (Figure 1a). To further reinforce this finding, we performed a two-hybrid luciferase assay in HEK293 cells overexpressing PINK1 and Bcl-xL, which confirmed a significant binding between the two proteins (Figure 1b). The interaction was also observed in SH-SY5Y cells stably expressing PINK1 after immunoprecipitation of endogenous Bcl-xL (Figure 1c). We could not detect any association between the two endogenous proteins in untreated cells, likely because of the very low levels of endogenous PINK1, which is rapidly processed by voltage-dependent mitochondrial proteases.[24] Conversely, the interaction between endogenous PINK1 and Bcl-xL was evident in cells treated with the mitochondrial uncoupler CCCP (Figure 1d), which is known to inhibit mitochondrial proteases, resulting in the selective accumulation of PINK1 on the surface of depolarized mitochondria.[18] Accordingly, in CCCP-treated SH-SY5Y cells, Bcl-xL strongly colocalized with PINK1 wt at the outer mitochondrial membrane; on the other hand, a PINK1 mutant lacking the mitochondrial target sequence (PINK1-ΔN) failed to accumulate on depolarized mitochondria and displayed impaired colocalization with Bcl-xL. Of note, Bcl-xL mainly colocalized with TOM20 even

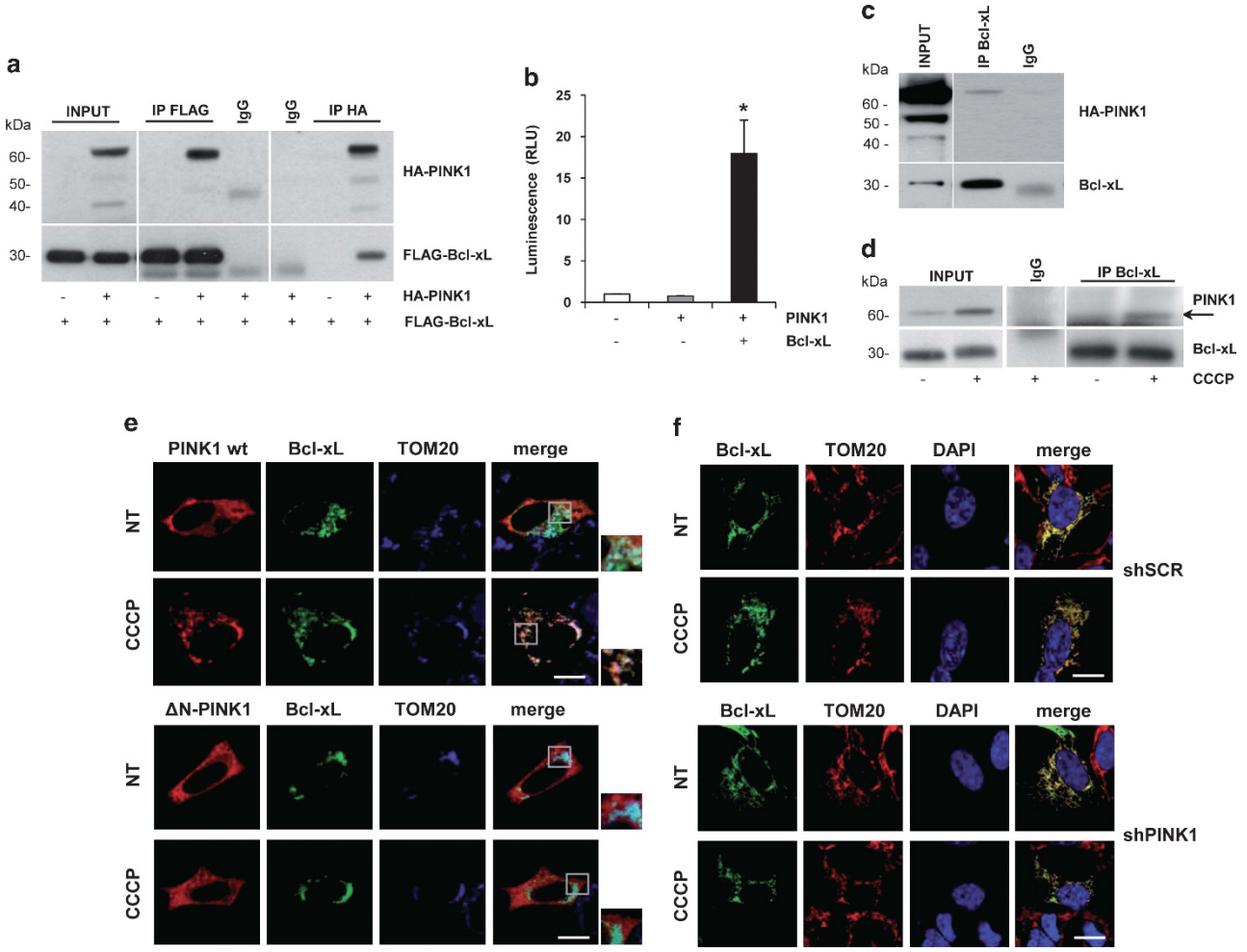

Figure 1 PINK1 interacts with Bcl-xL on depolarized mitochondria. (**a**) Reciprocal co-immunoprecipitations (co-IPs) of overexpressed PINK1 and Bcl-xL in HEK293 cells. PINK1 and Bcl-xL were immunoprecipitated with HA and FLAG antibodies, respectively. (**b**) Two-hybrid luciferase assay in HEK293 cells overexpressing PINK1 and Bcl-xL. HEK293 cells were transfected and processed as described in the Method section. In cells overexpressing both PINK1 and Bcl-xL, we observed a significant increase of luminescence compared with negative controls (Relative Light Units (RLU): 17.94 ± 4.03, $P = 0.026$). (**c**) co-IP of endogenous Bcl-xL and overexpressed PINK1 in SH-SY5Y cells. IP was performed with Bcl-xL antibody, followed by western blotting with HA antibody to detect PINK1. (**d**) co-IP of endogenous PINK1 and Bcl-xL. Lysates from SH-SY5Y cells, treated with CCCP or vehicle, were subjected to IP with Bcl-xL antibody, followed by immunoblotting with PINK1 antibody. (**e**) Colocalization of PINK1 and Bcl-xL at mitochondria. SH-SY5Y cells co-transfected with HA-PINK1 wt or ΔN and Bcl-xL–EGFP were treated with 6 h CCCP and subjected to confocal microscopy analysis. PINK1 was immunostained with HA antibody (red); TOM20 antibody was used to label the outer mitochondrial membrane (blue). Bcl-xL strongly colocalized with TOM20 in all experimental settings; conversely, PINK1 wt, but not PINK1-ΔN, colocalized with both Bcl-xL and TOM20 only in the presence of CCCP (see Supplementary Table S1 for overlap coefficients). (**f**) Colocalization of Bcl-xL and TOM20 upon PINK1 silencing. SH-SY5Y cells stably infected with scramble-shRNA (shSCR) or shPINK1 were transfected with Bcl-xL–EGFP and immunostained with TOM20 antibody (red). Merge pictures reveal colocalization. Bcl-xL strongly colocalized with TOM20 in all settings, regardless of PINK1 silencing (see Supplementary Table S2 for overlap coefficients). Scale bars: 10 μM

in untreated cells, and this was not affected by either CCCP exposure, overexpression of PINK1-ΔN (Figure 1e) or PINK1 knockdown (Figure 1f). The quantifications of colocalization relative to Figures 1e and f are presented in Supplementary Tables S1 and S2, respectively.

The interaction between PINK1 and Bcl-xL does not regulate mitophagy. It is well known that upon autophagy induction, the interaction between Bcl-xL and Beclin-1 is disrupted by either competitive binding or post-translational modifications, allowing Beclin-1 to activate the autophagy cascade.[22,25] Accordingly, we found that the Bcl-xL–Beclin-1 binding was clearly abolished in HEK293 cells subjected to nutrient deprivation, resulting in the activation of autophagy (Supplementary Figure S1a). We therefore hypothesized that the interaction between PINK1 and Bcl-xL observed upon CCCP treatment could selectively impair the Bcl-xL–Beclin-1 binding in the neighborhood of depolarized mitochondria, contributing to the mitophagy pathway.

To this end, we first performed co-immunoprecipitation experiments in CCCP-treated SH-SY5Y cells co-transfected with Bcl-xL and Beclin-1. However, no significant differences were observed in the association between the two proteins, despite a strong accumulation of LC3-II, indicative of activated autophagy (Figure 2a). The same result was obtained in HEK293 cells (Supplementary Figure S1b), and not even increasing amounts of PINK1 were able to disrupt the binding between Bcl-xL and Beclin-1 (Figure 2b).

Next, to evaluate whether Bcl-xL could have a role in mitophagy, wt or Parkin-inducible SH-SY5Y cells were infected with lentivirus expressing either scrambled- or Bcl-xL-shRNA. After CCCP treatment, we observed in both systems a significant decrease of mitochondrial markers by western blotting, which however remained unchanged in presence of Bcl-xL silencing (Figure 2c and d). Mitophagy was also assessed by confocal microscopy in Parkin-inducible SH-SY5Y cells; both Parkin recruitment at mitochondria and the number of cells with few or no mitochondria were unaltered by Bcl-xL downregulation (Figure 2e).

PINK1 phosphorylates Bcl-xL. To evaluate whether Bcl-xL could be a substrate of the PINK1 kinase activity, we first performed an *in vitro* mix beads kinase assay, which showed a significant four-fold increase of Bcl-xL phosphorylation by PINK1 (Figure 3a). We next explored the ability of endogenous Bcl-xL to be phosphorylated *in vivo*, in response to mitochondrial depolarization. To this end, SH-SY5Y cells were treated with either increasing concentrations of CCCP (up to 50 μM) or for different times (up to 24 h), followed by western blotting analysis with a phospho-specific Bcl-xL antibody directed against the phosphorylated serine 62. The levels of p-Bcl-xL progressively increased in the presence of higher CCCP concentrations as well as of longer time exposures (Figure 3b). To assess the specificity of the p-Bcl-xL antibody, we silenced Bcl-xL in SH-SY5Y cells treated with CCCP, and observed the disappearance of the corresponding signal on western blotting; the same result was obtained after treatment with the lambda protein phosphatase, while treatment with the positive control nocodazole produced a strong increase of p-Bcl-xL (Supplementary Figure S2), as previously reported.[26] In CCCP-treated SH-SY5Y cells, PINK1 silencing nearly abolished the levels of p-Bcl-xL (Figure 3c), confirming that phosphorylation was effectively dependent on PINK1. In line with this, overexpression of PINK1 wt, but not of the kinase-defective PINK1 KDD, was able to markedly increase the amount of p-Bcl-xL compared with cells expressing the empty vector (Figure 3d).

PINK1 protects cells against CCCP-induced apoptosis by phosphorylating Bcl-xL. As Bcl-xL is one of the most important pro-survival proteins, we asked whether the interaction between PINK1 and Bcl-xL could be involved in the regulation of apoptosis. To this end, we first infected SH-SY5Y cells with lentivirus expressing scrambled- or PINK1-shRNA (shPINK1), followed by CCCP treatment. Mitochondrial depolarization *per se* determined a marked decrease of cell viability, as revealed by the progressive accumulation of cleaved PARP, a well-known apoptotic marker. In this setting, PINK1 downregulation resulted in a significant increase of apoptotic cell death after 24 h treatment, as evidenced by a greater PARP cleavage compared with shSCR cells (Figure 4a). To confirm these findings, the effect of PINK1 depletion on CCCP-induced apoptosis was evaluated by FACS analysis (Figure 4b). In line with western blotting data, the proportion of apoptotic cells at 24 h was significantly higher in shPINK1 cells compared with control.

To evaluate whether CCCP-induced apoptosis could be reverted by PINK1 overexpression, shPINK1 cells were transfected with PINK1 wt or vector alone and then subjected to CCCP for 12 and 24 h. To test whether the kinase activity of PINK1 was required to protect from cell death, the ability of PINK1 KDD to rescue apoptosis was also analyzed. At 24 h, cleaved PARP levels, as well as the percentage of apoptotic cells measured by FACS, significantly decreased in presence of PINK1 wt compared with control cells, while cell viability was unaffected by overexpression of the PINK1 KDD mutant (Figures 4c and d). Moreover, we showed that, in Bcl-xL-silenced cells, PINK1 overexpression failed to protect against CCCP-induced apoptosis, suggesting that Bcl-xL acted downstream of PINK1 to promote cell survival (Figures 4e and f).

In order to link the protective function of PINK1 to Bcl-xL phosphorylation, PINK1-silenced cells were transfected with either phospho-defective (S62A) or phospho-mimicking (S62E) Bcl-xL constructs. Cleaved PARP levels and TUNEL-positive cells were significantly lower in presence of Bcl-xL S62E, which simulates Bcl-xL phosphorylation on serine 62, compared with both cells transfected with the Bcl-xL S62A mutant or the vector alone (Figures 4g and h).

PINK1-dependent phosphorylation of Bcl-xL impairs its pro-apoptotic cleavage. To explore how Bcl-xL phosphorylation by PINK1 might protects cells against CCCP-induced apoptosis, we asked whether mitochondrial depolarization was able to trigger the N-terminus cleavage of Bcl-xL, which is known to produce a pro-apoptotic fragment lacking the BH4 domain (ΔN-Bcl-xL),[27] and whether PINK1 could interfere with this process. To this aim, we silenced PINK1

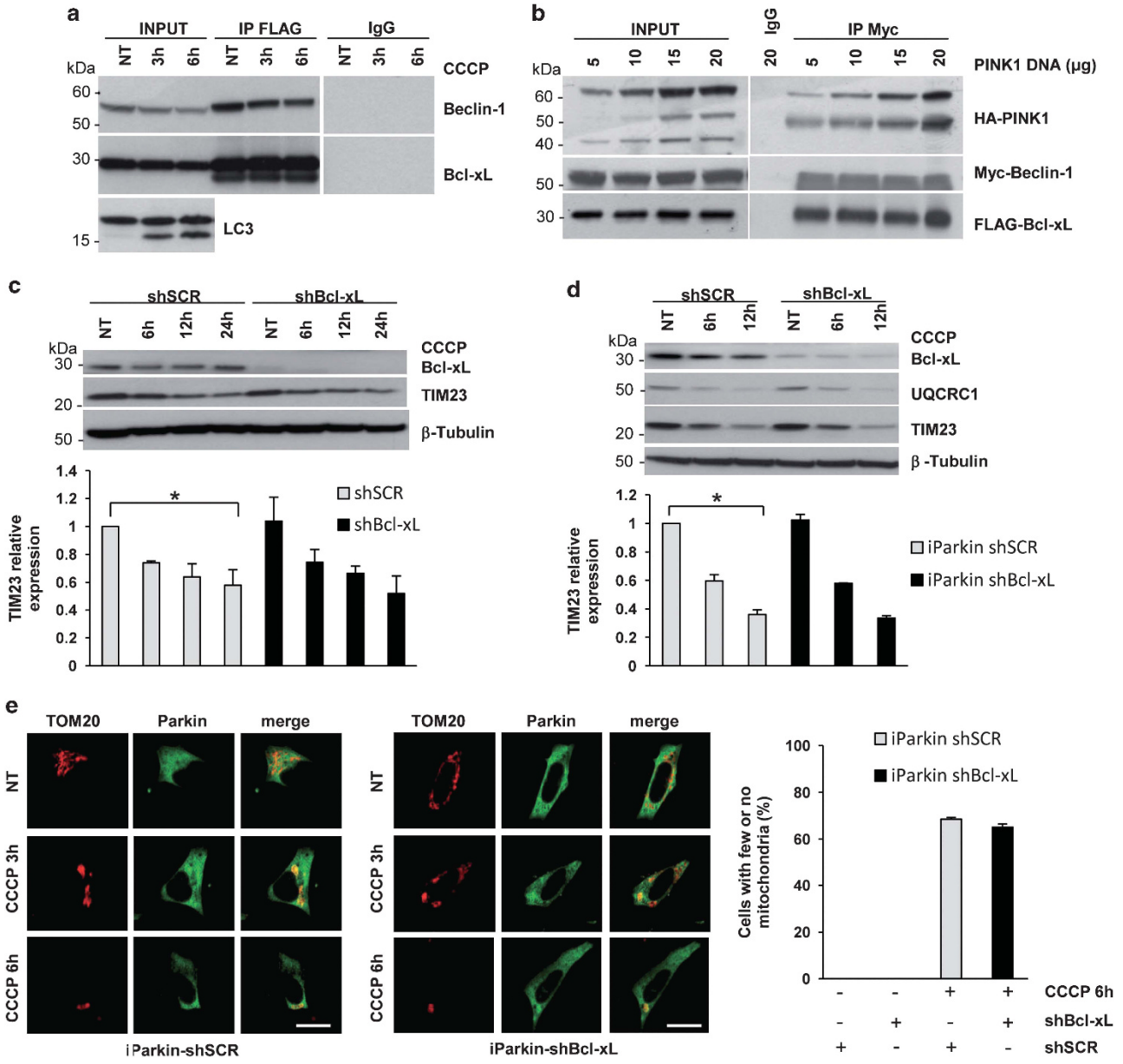

Figure 2 The interaction between PINK1 and Bcl-xL does not regulate mitophagy. (**a**) Bcl-xL–Beclin-1 co-IP in CCCP-treated SH-SY5Y cells. Bcl-xL was immunoprecipitated with FLAG antibody, followed by anti-Myc immunoblotting to detect Beclin-1. Autophagy activation was confirmed by LC3 western blotting. (**b**) Bcl-xL–Beclin-1 co-IP in HEK293 cells transfected with increasing amount of PINK1. Lysates were subjected to IP with Myc antibody, followed by immunoblotting with anti-FLAG. (**c** and **d**) Western blotting of mitochondrial markers in CCCP-treated wt and Parkin-inducible SH-SY5Y cells upon Bcl-xL silencing. Cells infected with either shSCR or Bcl-xL-shRNA (shBcl-xL) were treated with CCCP at the indicated times. Mitophagy was evaluated by assessing the decrease of the mitochondrial markers TIM23 and UQCRC1 by western blotting. Densitometric analysis revealed a significant decrease of TIM23 in both shSCR wt and Parkin-inducible SH-SY5Y cells treated with CCCP for 24 and 12 h, respectively (0.57 ± 0.11, $P = 0.033$ and 0.35 ± 0.03, $P = 0.0013$); however, we observed no significant differences in TIM23 levels related to Bcl-xL silencing (0.57 ± 0.11 *versus* 0.51 ± 0.12, $P = 0.67$ and 0.35 ± 0.03 *versus* 0.33 ± 0.01, $P = 0.47$).(**e**) Confocal microscopy analysis in CCCP-treated iParkin SH-SY5Y cells upon Bcl-xL silencing. Colocalization between Parkin (green) and TOM20 (red) was used as measure of mitophagy induction. Mitochondrial degradation was analyzed by counting the percentage of cells with few or no mitochondria after 6 h CCCP. Differences between shSCR and shBcl-xL cells were not significant (68.5 ± 0.70 *versus* 65.0 ± 1.41, $P = 0.09$). Scale bars: 10 μM. **P*-values < 0.05

in CCCP-treated SH-SY5Y cells overexpressing Bcl-xL, and found a marked increase of ΔN-Bcl-xL (Figure 5a). Further reinforcing this result, PINK1 knockdown significantly enhanced the cleavage of endogenous Bcl-xL (Figure 5b).

In order to analyze whether the kinase activity of PINK1 was required to protect Bcl-xL from its cleavage, shPINK1 cells were transfected with either PINK1 wt or KDD or empty vector, and then exposed to CCCP. Overexpression of PINK1 wt, but not of the KDD mutant, determined a significant reduction of ΔN-Bcl-xL compared with control cells (Figure 5c). Finally, the accumulation of cleaved Bcl-xL was also significantly reduced in presence of the phospho-mimicking Bcl-xL S62E compared

with the phospho-defective Bcl-xL S62A construct (Figure 5d). These data suggest that PINK1-dependent Bcl-xL phosphorylation on serine 62 could protect from CCCP-induced apoptosis by hampering the Bcl-xL N-terminal cleavage (Figure 6).

Discussion

Besides its established role in regulating mitochondrial dynamics and homeostasis, we recently showed that PINK1 interacts with Beclin-1 and is able to promote basal and starvation-induced autophagy.[20] To further explore this path-

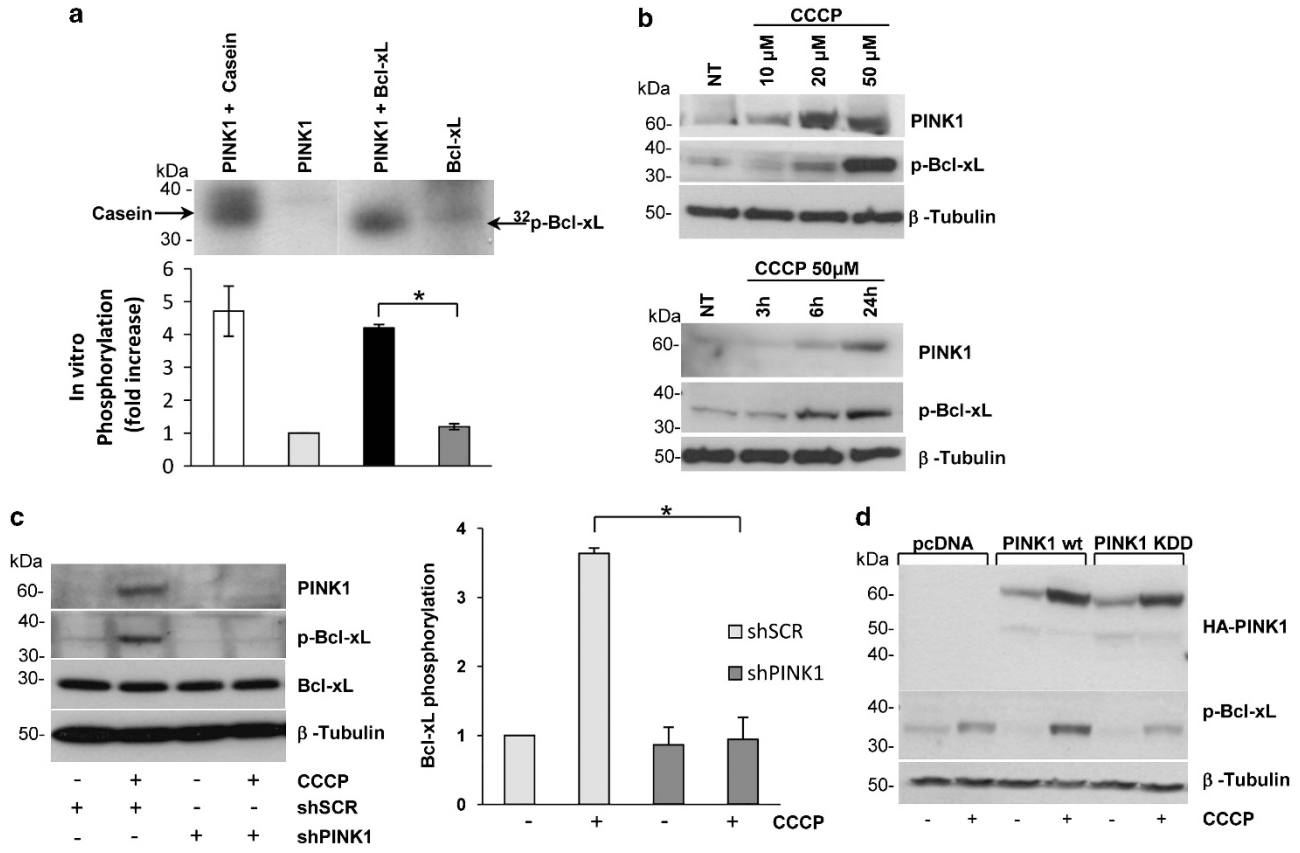

Figure 3 PINK1 phosphorylates Bcl-xL. (**a**) Mix beads *in vitro* kinase assay. Immunopurified PINK1 and Bcl-xL were processed as described in the Methods section. Casein was used as a positive control of the PINK1 kinase activity. PINK1 and Bcl-xL alone were used as negative controls. Bcl-xL phosphorylation significantly increased in the presence of PINK1 (4.12 ± 0.10, $P = 0.001$). (**b**) *In vivo* phosphorylation of endogenous Bcl-xL. SH-SY5Y cells were either subjected to increasing concentration of CCCP (upper panel) or treated with 50 μM CCCP up to 24 h (lower panel). Lysates were processed for western blotting using p-Bcl-xL and PINK1 antibodies. (**c**) Bcl-xL phosphorylation upon PINK1 silencing. Lysates from SH-SY5Y cells infected with either shSCR or shPINK1 were treated with 50 μM CCCP for 24 h. PINK1 silencing and p-Bcl-xL levels were assessed by immunoblotting. Densitometric analysis revealed a significant reduction of p-Bcl-xL in CCCP-treated shPINK1 cells compared with control (0.95 ± 0.31 *versus* 3.63 ± 0.08, $P = 0.007$). (**d**) Bcl-xL phosphorylation after overexpression of PINK1. Lysates from CCCP-treated SH-SY5Y cells transfected with vector alone (pcDNA), PINK1 wt or KDD were processed for western blotting using HA and p-Bcl-xL antibodies. **P*-values < 0.05

Figure 4 The interaction between PINK1 and Bcl-xL protects against CCCP-induced apoptosis. (**a** and **b**) Apoptosis evaluation upon PINK1 silencing. Either shSCR or shPINK1 cells were treated with CCCP followed by cleaved PARP immunoblotting (**a**) or FACS analysis (**b**). Densitometric analysis on cleaved PARP revealed, at 24 h CCCP, a significant increase of cell death in shPINK1 cells compared with control (5.78 ± 1.21 *versus* 3.34 ± 0.92, $P = 0.03$). The percentage of TUNEL-positive cells at 24 h was also significantly higher in shPINK1 compared with shSCR cells (28.47 ± 0.66 *versus* 19.38 ± 0.55, $P = 0.04$).(**c** and **d**) Apoptosis rescue by PINK1. shPINK1 cells were transfected with PINK1 wt or KDD or vector alone (pcDNA). After 24 h CCCP, cleaved PARP levels were significantly lower in presence of PINK1 wt compared with both empty vector (3.86 ± 0.08 *versus* 5.34 ± 0.07, $P = 0.003$), and KDD (5.37 ± 0.45, $P = 0.042$). The proportion of TUNEL-positive cells also significantly decreased in presence of PINK1 wt compared with both control (16.79 ± 0.81 *versus* 25.40 ± 0.68, $P = 0.009$), and KDD (22.77 ± 0.27, $P = 0.02$). (**e** and **f**) Apoptosis evaluation in Bcl-xL-silenced cells after PINK1 overexpression. SH-SY5Y cells subjected to Bcl-xL knockdown were transfected with PINK1 wt or empty vector (pcDNA) and then treated with CCCP for 24 h. Upon mitochondrial depolarization, the increase of cleaved PARP levels in PINK1 overexpressing cells was similar to that observed in cells transfected with the empty vector (3.54 ± 0.61 *versus* 3.37 ± 0.57, $P = 0.85$); the same result was obtained analyzing the percentage of TUNEL-positive cells by FACS (47.56 ± 2.51 *versus* 49.28 ± 2.47, $P = 0.82$). (**g** and **h**) Apoptosis rescue by Bcl-xL S62E. shPINK1 cells were transfected with Bcl-xL S62E or S62A, or with the empty vector. At 24 h CCCP, cleaved PARP levels were significantly lower in presence of Bcl-xL S62E compared with both Bcl-xL S62A (2.76 ± 0.55 *versus* 4.03 ± 0.50, $P = 0.042$) and empty vector (4.87 ± 0.81, $P = 0.02$). Similarly, the percentage of TUNEL-positive cells was significantly lower in shPINK1 cells transfected with Bcl-xL S62E compared with both Bcl-xL S62A (13.76 ± 0.13 *versus* 18.41 ± 0.35, $P = 0.003$) and vector alone (24.48 ± 0.73, $P = 0.0008$). **P*-values < 0.05

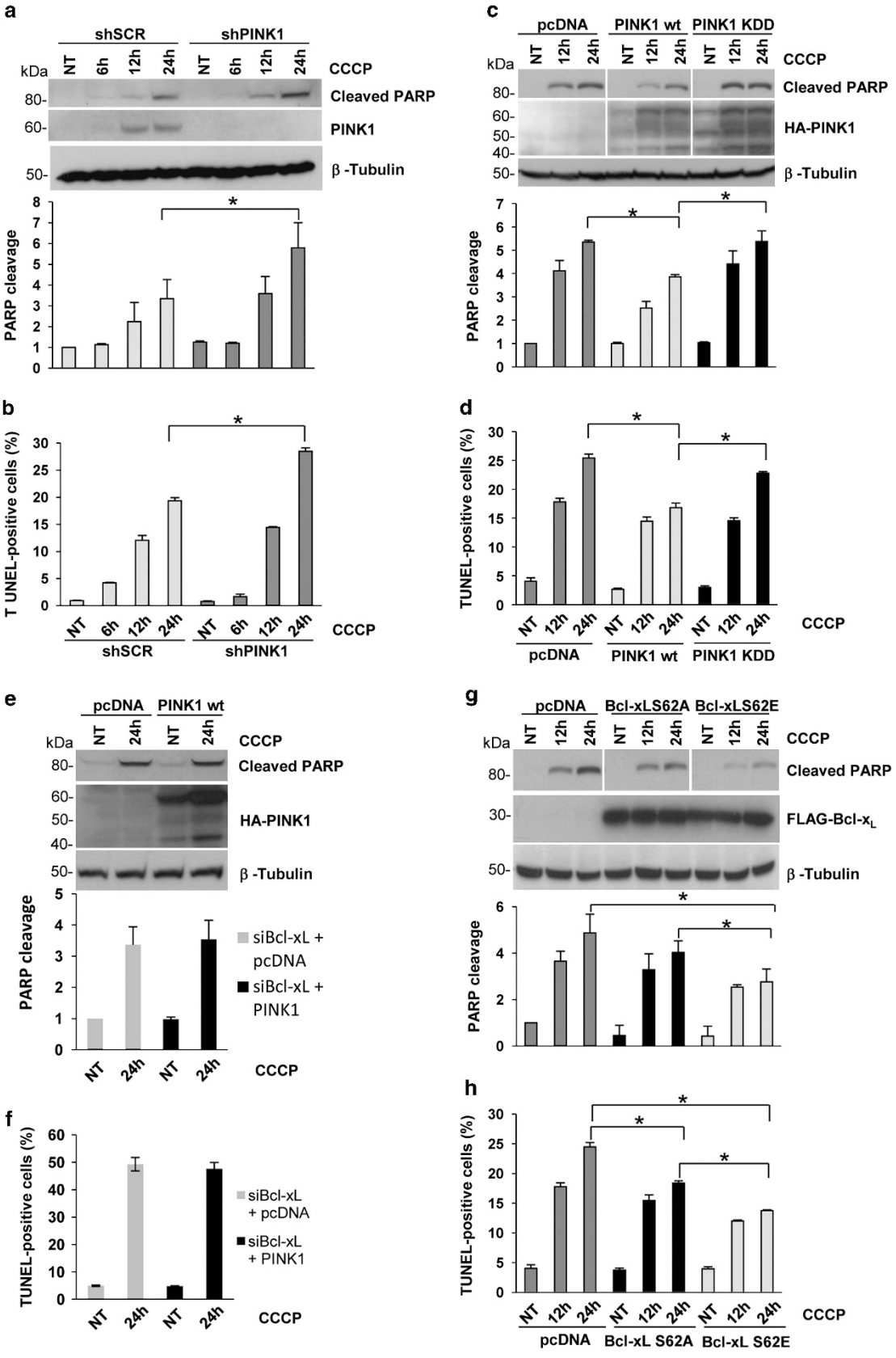
a
shSCR
shPINK1
kDa
NT
6h
12h
24h
CCCP
80-
Cleaved PARP
60-
PINK1
50-
β -Tubulin
PARP cleavage
b
T UNEL-positive cells (%)
shSCR
shPINK1
c
pcDNA
PINK1 wt
PINK1 KDD
HA-PINK1
d
TUNEL-positive cells (%)
e
FLAG-PINK1
siBcl-xL + pcDNA
siBcl-xL + PINK1
f
g
Bcl-xLS62A
Bcl-xLS62E
FLAG-Bcl-xL
h
Bcl-xL S62A
Bcl-xL S62E

way, we focused on members of the Beclin-1 multiprotein complex, and found that PINK1 specifically interacts with Bcl-xL, a main anti-apoptotic protein of the Bcl-2 family. On the other hand, we failed to detect any association between PINK1 and the anti-apoptotic member Bcl-2 (data not shown).

Despite we found a strong interaction between over-expressed PINK1 and Bcl-xL, the binding between the two endogenous protein was undetectable in healthy cells, probably because PINK1 is actively and continuously cleaved by voltage-dependent mitochondrial proteases.[24] Indeed, other groups also failed to demonstrate the interaction between endogenous PINK1 and other binding partners such as Parkin or Miro in basal conditions.[17,19] Conversely, the interaction between endogenous PINK1 and Bcl-xL was observed in cells treated with the mitochondrial uncoupler CCCP, that inhibits mitochondrial proteases and induces a robust accumulation of PINK1 at the outer membrane of depolarized mitochondria.[16–18] In line with this, Bcl-xL colocalization with a PINK1 mutant lacking the mitochondrial target sequence was dramatically reduced, indicating that the PINK1–Bcl-xL binding mostly happens at the mitochondrial surface. These findings imply that PINK1 interacts with Bcl-xL only upon its selective accumulation on depolarized mitochondria, suggesting a specific role for this interaction in counteracting mitochondrial damage.

In addition to its well-characterized anti-apoptotic function, Bcl-xL is also known to inhibit autophagy by sequestering Beclin-1; in HeLa cells, disruption of this association by either competitive binding or post-translational modifications is known to release Beclin-1, leading to autophagosome formation and activation of the autophagy cascade.[22,25] In light of these observations, we hypothesized that the interaction between PINK1 and Bcl-xL could serve to disrupt the Bcl-xL–Beclin-1 binding in the proximity of depolarized

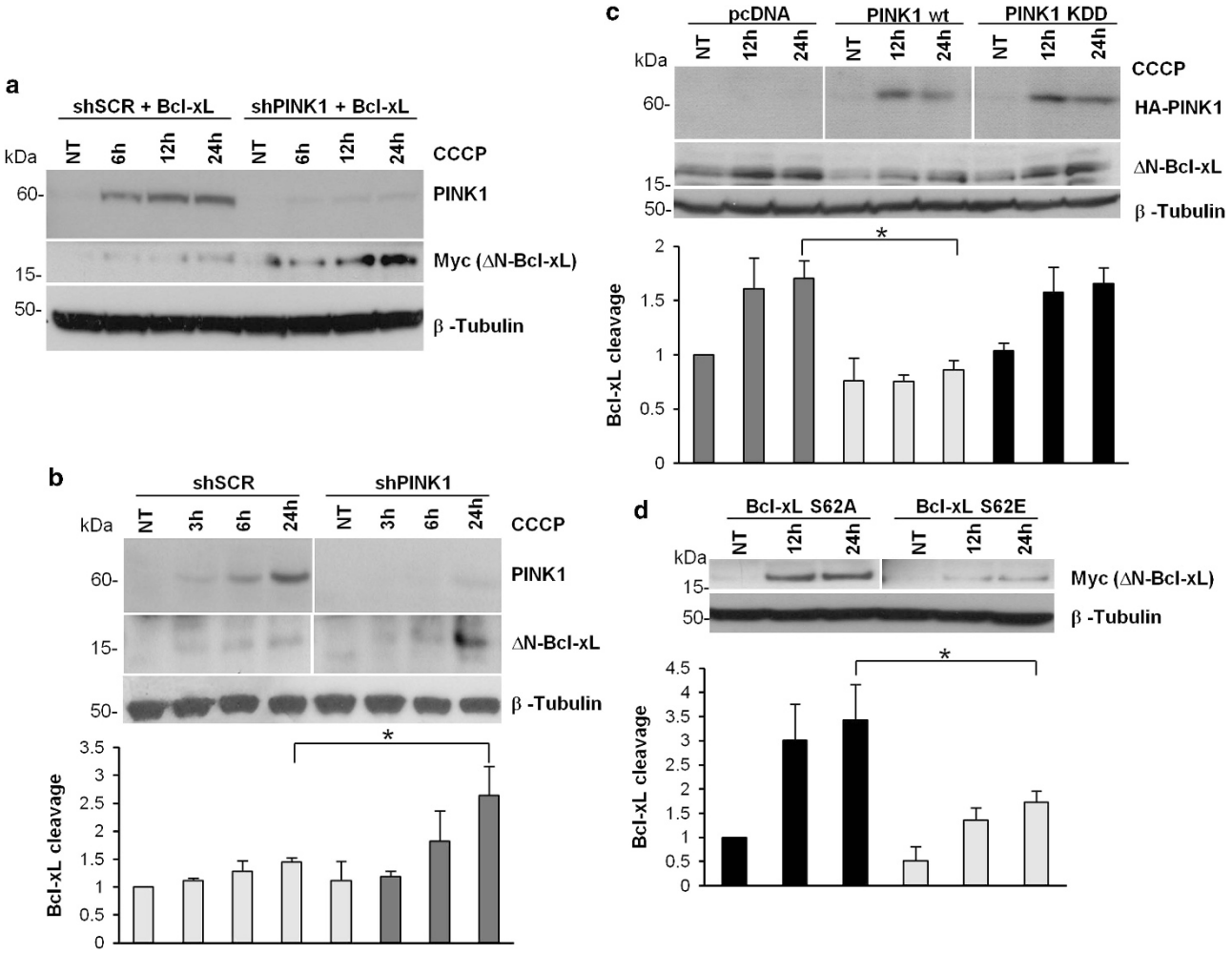

Figure 5 PINK1-dependent Bcl-xL phosphorylation impairs Bcl-xL cleavage. (**a** and **b**) ΔN-Bcl-xL formation upon PINK1 silencing. Lysates from shSCR or shPINK1 cells, either transfected with Myc-Bcl-xL (**a**) or untransfected (**b**), were treated with CCCP and processed for western blotting. The cleavage of overexpressed Bcl-xL was well evident upon mitochondrial depolarization in PINK1-silenced cells (**a**). The endogenous levels of ΔN-Bcl-xL also significantly increased at 24 h CCCP in shPINK1 compared with shSCR cells (2.63 ± 0.52 *versus* 1.44 ± 0.07, $P = 0.017$). (**c**) Rescue of Bcl-xL cleavage by PINK1. shPINK1 cells were transfected with PINK1 wt or KDD or vector alone (pcDNA). After 24 h CCCP, cleaved endogenous Bcl-xL was significantly reduced in presence of PINK1 wt compared with both control (0.85 ± 0.09 *versus* 1.70 ± 0.15, $P = 0.022$) and KDD (1.65 ± 0.14, $P = 0.022$). (**d**) Cleavage of Bcl-xL S62E and S62A. Lysates from CCCP-treated shPINK1 cells transfected with the indicated Bcl-xL constructs were processed for immunoblotting. Cleaved Bcl-xL was detected using the Myc antibody. At 24 h CCCP, cleavage was significantly reduced in presence of Bcl-xL S62E compared with S62A (1.72 ± 0.23 *versus* 3.43 ± 0.72, $P = 0.018$). *P-values < 0.05

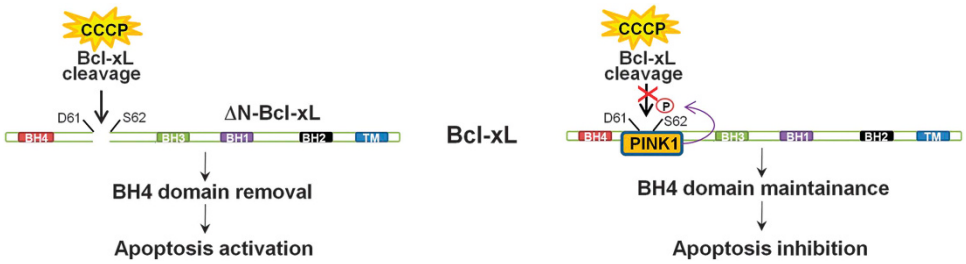

Figure 6 Schematic model of the mechanism through which PINK1–Bcl-xL interaction could protect against cell death induced by mitochondrial depolarization. Mitochondrial depolarization induces cleavage of Bcl-xL at the aspartate 61 (D61). The resulting C-terminal fragment (ΔN-Bcl-xL) lacks the anti-apoptotic N-terminal BH4 domain and is a potent inducer of cell death. PINK1 phosphorylates the serine 62 (S62) of Bcl-xL, impairing cleavage at the adjacent D61 site. In this way, the BH4 domain of Bcl-xL is maintained and the full-length protein can exert its anti-apoptotic function

mitochondria, contributing to their selective removal through the mitophagy pathway. However, CCCP treatment, as well as PINK1 overexpression, were not able to induce loss of Bcl-xL–Beclin-1 interaction either in SH-SY5Y or in HEK293 cells, suggesting that this mechanism does not have a role in mitophagy. Accordingly, we showed that Bcl-xL is not required for Parkin recruitment on depolarized mitochondria and mitophagy activation, indicating that the functional significance of the PINK1–Bcl-xL interaction is independent from the role of the PINK1–Parkin axis in regulating mitochondrial degradation.

Further studies are required to explore the pathways of CCCP-induced autophagy, as shown by LC3-II accumulation in SH-SY5Y cells. A possible explanation could be the activation of a Beclin-1 independent mechanism (non-canonical autophagy), as previously reported for other pro-apoptotic compounds such as staurosporine, H_2O_2 and MPP^+.[28]

With the present study, we demonstrated for the first time that PINK1 is able to directly phosphorylate Bcl-xL both *in vitro* and *in vivo*. Our results point to serine 62 of Bcl-xL as the main phosphorylation site. Interestingly, levels of phosphorylated Bcl-xL strongly increased with protracted exposures of CCCP, suggesting a direct correlation with the duration of mitochondrial depolarization. In this setting, PINK1 downregulation or overexpression of a kinase-defective mutant dramatically reduced p-Bcl-xL levels.

Of note, we failed to detect phosphorylation of Bcl-xL at the serine 62 following treatment with diverse apoptotic stimuli, such as proteasome inhibition by MG132, 6-OHDA exposure, nutrient deprivation or staurosporine, likely because none of these compounds is able to determine a significant accumulation of endogenous PINK1-FL at mitochondria (Supplementary Figure S3).

To date, available experiments on the functional role of phosphorylated Bcl-xL are quite controversial; some studies have reported that Bcl-xL phosphorylation impairs its anti-apoptotic function, likely by disrupting the binding with the pro-apoptotic protein Bax;[29] in contrast, other groups have demonstrated that p-Bcl-xL shows increased stability and enhanced pro-survival activity, whereas dephosphorylation of Bcl-xL may trigger apoptosis.[30–32]

Here, we report that PINK1 is required to protect cells from CCCP-induced apoptosis, and that such protection strongly depends on its ability to interact with Bcl-xL and to phosphorylate its serine 62. In fact, we observed absence of protection by PINK1 in cells subjected to Bcl-xL silencing and, conversely, rescue from apoptosis by a Bcl-xL mutant that mimics the phosphorylation on the S62, confirming that Bcl-xL represents a downstream target of PINK1 kinase activity.

The anti-apoptotic function of Bcl-xL is exerted through two main pathways, both implicated in the modulation of mitochondrial membrane permeability.[33] On one hand, Bcl-xL is known to sequester pro-apoptotic molecules such as Bax, leading to its continuous retrotranslocation from mitochondria to cytosol.[34] Indeed, in CCCP-treated SH-SY5Y cells, we found a robust interaction between endogenous Bcl-xL and Bax, which however, remained unchanged after PINK1 silencing (data not shown).

The other known anti-apoptotic pathway of Bcl-xL implies the inhibition of the voltage-dependent anion channel activity, that results in preservation of the mitochondrial membrane potential and blockage of cytochrome c release. This function is directly mediated by the N-terminal BH4 domain of Bcl-xL, which was shown to be essential for preventing cell death.[35] In line with this, apoptotic stimuli such as hypoxia/ischemia were found to induce the cleavage of Bcl-xL at the aspartate 61, generating a C-terminal fragment (ΔN-Bcl-xL) that potently stimulated apoptosis.[27] Moreover, we recently showed that knock-in mice expressing non-cleavable Bcl-xL exhibited a reduced vulnerability to ischemia-induced neuronal death.[36] Here, we found that the pro-apoptotic cleavage of Bcl-xL is also triggered by mitochondrial depolarization, and the amount of ΔN-Bcl-xL strongly increases in the absence of PINK1. Intriguingly, we noticed that the cleavage site of Bcl-xL at aspartate 61 is just adjacent to the serine 62 phosphorylated by PINK1. This observation suggested that phosphoserine 62 could protect from CCCP-induced apoptosis by hampering the production of the ΔN-Bcl-xL fragment, for instance through a steric or electrostatic hindrance to the cleavage site.[37] Consistent with this, we showed that Bcl-xL cleavage in PINK1-silenced cells was clearly reduced in presence of the Bcl-xL construct mimicking phosphorylation on serine 62.

These findings highlight a novel pathway through which PINK1 might exert its neuroprotective activity; moreover, the identification of Bcl-xL as a PINK1 substrate opens a novel intriguing scenario to further assess the biological role of PINK1 not only in PD but also in cancer, where the pro-survival activity of Bcl-xL is already well characterized.[33] Low cancer rates have been reported in patients with PD,

suggesting that common genes and pathways might be implicated in both diseases.[38] PINK1 was identified for the first time through a gene expression screening in ovarian carcinoma cells overexpressing PTEN, a key tumor suppressor gene, which is mutated in several malignancies.[39] Recent data have proposed a novel function of PINK1 in promoting carcinogenesis, insofar PINK1 silencing was shown to downregulate Bcl-xL expression in bladder cancer cells, sensitizing them to ROS-mediated cell death.[40–41] In this light, our finding of a direct role of PINK1 in promoting Bcl-xL phosphorylation could not only be relevant for neuroprotection, but also represent a potential molecular target for cancer treatment.

Materials and Methods

Eukaryotic expression vectors and shRNA constructs. The PINK1 constructs were all tagged at the C-terminus with the HA epitope. PINK1 wt and PINK1 112-581(PINK1 ΔN), as well as the Myc-tagged Beclin-1 construct have been described previously.[20] The putative kinase-defective PINK1 K219A, D362A, D384A triple mutant (PINK1 KDD) was generated from PINK1 wt cDNA by using the QuikChange II XL Site-Directed Mutagenesis Kit (Stratagene, La Jolla, CA, USA). The Bcl-xL construct tagged with FLAG epitope at the N-terminus (pcDNA-Bcl-xL) was kindly provided by Prof. Del Bufalo (Experimental Chemotherapy Laboratory, Regina Elena National Cancer Institute, Rome, Italy). The pEGFP–Bcl-xL vector used in immunofluorescence experiments was generated by inserting full-length Bcl-xL into the BglII restriction site of pEGFP-C1 (Clontech, Mountain View, CA, USA). To assess the N-terminal cleavage of Bcl-xL, a construct tagged at the C-terminus with the Myc epitope (pCMV6-Bcl-xL) was purchased by OriGene (Rockville, MD, USA). The phospho-deficient Bcl-xL S62A and the phospho-mimicking Bcl-xL S62E constructs were produced by site-specific mutagenesis.

For the two-hybrid luciferase assay, the start codon of pcDNA-PINK1 was removed by site-specific mutagenesis and replaced with a BamHI restriction site; similarly, the start codon of pCMV6-Bcl-xL was replaced with a BglII restriction site. The PINK1 ORF was digested with BamHI/XhoI and cloned into the pACT vector (Promega, Fitchburg, WI, USA), digested with BamHI/SalI. The Bcl-xL ORF was digested with BglII/XhoI and cloned into the pBIND vector (Promega), digested with BamHI/SalI. All constructs were verified by direct sequencing.

To knockdown PINK1 and Bcl-xL expression in SH-SY5Y cells (shPINK1 and shBcl-xL), pMISSION validated shRNA bacterial glycerol stocks were purchased from Sigma-Aldrich (St Louis, MO, USA) (PINK1 clone ID: NM_032409.1-548s1c1; Bcl-xL clone ID: NM_001191.2-857s1c1). The MISSION pLKO.1-puro scrambled shRNA was used as negative control (shSCR). pMISSION-gagpol and pMISSION-vsvg were used as packaging constructs. The corresponding plasmids were purified from JM109 strain and used to generate lentiviral particles in 293T packaging cells.

Cell cultures. HEK293, 293T and SH-SY5Y cells were maintained in Dulbecco's modified Eagle's medium (DMEM; Life Technologies, Carlsbad, CA, USA), supplemented with 2 mM *L*-glutamine, 200 U/ml penicillin, 200 mg/ml streptomycin, 1 mM sodium pyruvate and 10% heat inactivated FBS at 37 °C in 95% humidifier air and 5% CO_2.

Parkin-inducible SH-SY5Y cells, kindly provided by Dr. Wolfdieter Springer and Prof. Philippe J Kahle (Laboratory of Functional Neurogenetics, Department for Neurodegenerative Diseases, Hertie Institute for Clinical Brain Research, University of Tübingen, Germany), were cultured in DMEM/HAM F12 1 : 1 (Life Technologies) containing 10% Tetracycline-free FBS (Clontech), 7 μg/ml Blasticidin and 300 μg/ml Zeocin (both from Life Technologies). Parkin expression was induced by adding 1 μg/ml Doxicycline (Sigma-Aldrich) for 48 h.[17]

Transfections and infections. HEK293 and 293T cells were transfected with the calcium phosphate method. SH-SY5Y cells were transfected with Lipofectamine 2000 reagent (Life Technologies). Stable transfectants expressing PINK1 wt were produced as previously described.[20]

To downregulate PINK1 and Bcl-xL, either wt or Parkin-inducible SH-SY5Y cells were infected overnight with the viral supernatant, in presence of 8 μg/ml Polybrene (Sigma-Aldrich). Stable transductants were obtained by adding 2 μg/ml Puromycin (Sigma-Aldrich) up to 10 days.

Treatments. For experiments of mitochondrial depolarization, both HEK293 and SH-SY5Y cells were exposed to 50 μM CCCP (Sigma-Aldrich) or vehicle (DMSO) at the indicated times. Starvation was obtained by culturing cells in serum-free Earle's Balanced Salt Solutions medium (Life Technologies). The microtubules-inhibitor nocodazole (200 μM) (Sigma-Aldrich) was used as positive control of Bcl-xL phosphorylation.

Antibodies. The following antibodies were used for immunoprecipitation, western blotting and immunofluorescence assays: mouse anti-FLAG (clone M2, Sigma-Aldrich), mouse anti-HA (Sigma-Aldrich), rat anti-HA (Roche Applied Science, Penzberg, Germany), rabbit anti-HA (Sigma-Aldrich), rabbit anti-Bcl-xL (Cell Signaling Technologies, Danvers, MA, USA), mouse anti-Myc (Santa-Cruz Biotechnology, Santa Cruz, CA, USA), goat anti-Myc (Novus Biologicals, Littleton, CO, USA), rabbit anti-PINK1 (Novus Biologicals), mouse anti-UQCRC1 (Santa-Cruz, Biotechnology), mouse anti-TIM23 (BD Biosciences, San Jose, CA, USA), mouse anti-TOM20 (BD Biosciences), mouse anti-Parkin (Santa-Cruz, Biotechnology), rabbit anti-phospho-Ser62-Bcl-xL (Santa-Cruz, Biotechnology), mouse anti-β-tubulin (Sigma-Aldrich), rabbit anti-LC3B (Sigma-Aldrich), rabbit anti-cleaved PARP (Cell Signaling Technologies), and chicken anti-ΔN-Bcl-xL (Aves Labs, Tigard, OR, USA). HRP-conjugated secondary antibodies were: anti-Mouse and anti-Rabbit (both from GE Healthcare, Little Chalfont, UK), anti-Rat (Life Technologies), anti-Goat (Bio-Rad, Hercules, CA, USA) and anti-Chicken (Sigma-Aldrich). Secondary antibodies used in immunofluorescence experiments were conjugated with either Alexa Fluor 488, Alexa Fluor 555 or Alexa Fluor 405 (Life Technologies).

Coimmunoprecipitation assays. HEK293 and SH-SY5Y cells, exposed or not at the indicated stress, were lysed in IP buffer (20 mM Hepes, 120 mM NaCl, 1% Triton-X100) containing protease and phosphatase inhibitors (Thermo Fisher Scientific, Waltham, MA, USA). IP were performed by incubating 500 μg of the whole-cell lysates (INPUT) with the indicated antibodies overnight at 4 °C. Mouse or rabbit IgG were used as controls of non-specific co-immunoprecipitation.

The following day, protein A- or G- beads (Sigma-Aldrich) were added and incubated for 6 h at 4 °C. The immunocomplexes were then washed 3 times with lysis buffer, resuspended in SDS sample buffer (Life Technologies), and finally processed for western blotting.

Two-hybrid luciferase assay. The assay was performed by using the CheckMate Mammalian Two-Hybrid System (Promega). Briefly, HEK293 cells were co-transfected with the following vectors: pACT-PINK1 + pBIND-Bcl-xL + pG5*luc* were used to analyze the interaction between PINK1 and Bcl-xL; pACT-empty + pBIND-empty + pG5*luc* and pACT-PINK1 + pBIND-empty + pG5*luc* were used as negative controls. The expression of VP16-PINK1 and GAL4-Bcl-xL fusion proteins was verified by Western blotting. 48 h after transfection, lysates were processed according to the Dual-Luciferase Reporter Assay System (Promega) and luciferase activity measured by using a MicroLumat Plus Microplate Luminometer LB96V (Berthold Technologies). Luminescence values, expressed as Relative Light Units, were obtained from at least three independent experiments and displayed as mean ± S.E.M. Renilla luciferase was used as normalizing transfection control.

***In vitro* mix beads kinase assay.** Lysates from HEK293 cells transiently transfected with either PINK1 and Bcl-xL, were subjected to IP with HA and FLAG antibody (Sigma-Aldrich) respectively, and a mixed beads kinase assay was performed as described previously.[42] Briefly, immunopurified Bcl-xL protein was washed four times with IP buffer and once with kinase reaction buffer (20 mM Hepes, pH 7.5, 20 mM $MgCl_2$, 25 mM β-glycerophosphate, 2 mM DTT, and 100 μM sodium orthovanadate), before being combined with immunopurified PINK1 and incubated in a 20 μl final volume of kinase reaction buffer containing 5 μCi γ-[^{32}P]ATP (PerkinElmer) at 30 °C for 30 min. Reaction was stopped by addition of 4X SDS sample buffer and boiled for 10 min. [^{32}P]-labeled reaction products were resolved on SDS-polyacrylamide gel electrophoresis (SDS-PAGE) and analyzed by autoradiography.

Treatment with lambda phosphatase. Lysates from SH-SY5Y cells treated with CCCP for different times were subjected to SDS-PAGE. Two identical sets of extract aliquots were run in parallel on the same gel. Following transfer to a nitrocellulose membrane, the blot was cut in two halves: one half was treated with lambda protein phosphatase (New England Biolabs, Ipswich, MA, USA), whereas

the other half was used as a non-treated control.[43] Matched phosphatase-treated and control sets of lanes were then probed with p-Ser62-Bcl-xL antibody.

Western blotting analysis. Cells were lysed in RIPA buffer (Cell Signaling) containing protease and phosphatase inhibitors and protein extracts were quantified by using the bicinchoninic acid (BCA) assay (Thermo Fisher Scientific). Lysates (50 μg) were subjected to SDS-PAGE, probed with the primary and secondary antibodies listed above, and detected by using ECL-Plus Western Blotting Detection System (GE Healthcare). All experiments were normalized by β-tubulin expression. Image contrast and brightness and densitometry measurements were performed in Adobe Photoshop CS2 (Adobe Systems Incorporated, San Jose, CA, USA). In all panels, values are plotted as fold-change relative to control, which has been set to a value of 1.

Immunofluorescence and confocal microscopy. Immunofluorescence analysis was performed as described previously.[20] Images were acquired by using the confocal microscope PCM Eclipse TE300 or the C2 Confocal Microscopy System (both from Nikon Instruments, Tokyo, Japan). Merged images were obtained with EZ2000 or NIS Element software. Quantification of colocalization, expressed in terms of overlap coefficient (R), was calculated on several randomly selected cells from different slides by using the WCIF ImageJ software (www.uhnresearch.ca/facilities/wcif/imagej/).

Mitophagy assessment. Either wt or Parkin-inducible SH-SY5Y cells were infected with scrambled- or Bcl-xL-shRNA and then treated with CCCP at the indicated times. Parkin recruitment at mitochondria was assessed by colocalization experiments with the outer mitochondrial membrane marker TOM20. Mitophagy induction was calculated by counting cells with few or no mitochondria. The decrease of TIM23 (inner mitochondrial membrane) and UQCRC1 (mitochondrial matrix) levels was evaluated by western blotting, and quantified by densitometric analysis.

FACS analysis. Cells were washed in PBS and fixed in 70% ethanol overnight at 4 °C. The next day, samples were washed in PBS + 1% BSA and then processed according to the TUNEL-based 'In Situ Cell Death Detection Kit Fluorescein' (Roche Diagnostic, Basel, Switzerland), in conjunction with propidium iodate staining. Single-cell suspensions were analyzed by Cyan ADP (Beckman Coulter, Brea, CA, USA). Apoptosis was scored by quantifying the population of TUNEL- and propidium iodate-positive cells. Flow-cytofluorimetric data were plotted and analyzed by using the Summit 4.3 software (Beckman Coulter).

Statistical analysis. Densitometric results, counts at confocal microscopy and cytofluorimetric data were represented as histograms; values were obtained from at least three independent experiments and expressed as means ± S.E.M. Statistical analysis was carried out by using unpaired two-tailed Student's *t*-test, with *P*-values < 0.05 considered as significant.

Conflict of Interest

The authors declare no conflict of interest.

Acknowledgements. We are grateful to Prof. M Piacentini and Dr. GM Fimia (National Institute for Infectious Diseases Lazzaro Spallanzani IRCCS, Rome) for their helpful suggestions. This work was supported by grants from the Italian Ministry of Health (Ricerca Corrente 2012, Ricerca Finalizzata 2008, Bando Giovani Ricercatori 2009), the Italian Telethon Foundation (GGP10140) and the Italian Ministry of Instruction, University and Research (Bando FIRB Accordi di Programma 2010).

1. Siderowf A, Stern M. Update on Parkinson disease. *Ann Intern Med* 2003; **138**: 651–658.
2. Schapira AH. Mitochondria in the etiology and pathogenesis of Parkinson's disease. *Lancet Neurol* 2008; **7**: 97–109.
3. Belin AC, Westerlund M. Parkinson's disease: a genetic perspective. *FEBS J* 2008; **275**: 1377–1383.
4. Deas E, Plun-Favreau H, Gandhi S, Desmond H, Kjaer S, Loh S *et al.* PINK1 cleavage at position A103 by the mitochondrial protease PARL. *Hum Mol Genet* 2011; **20**: 867–879.
5. Jin SM, Lazarou M, Wang C, Kane LA, Narendra DP, Youle RJ. Mitochondrial membrane potential regulates PINK1 import and proteolytic destabilization by PARL. *J Cell Biol* 2010; **191**: 933–942.
6. Silvestri L, Caputo V, Bellacchio E, Atorino L, Dallapiccola B, Valente EM *et al.* Mitochondrial import and enzymatic activity of PINK1 mutants associated to recessive parkinsonism. *Hum Mol Genet* 2005; **14**: 3477–3492.
7. Valente EM, Abou-Sleiman PM, Caputo V, Muqit MM, Harvey K, Gispert S *et al.* Hereditary early-onset Parkinson's disease caused by mutations in PINK1. *Science* 2004; **304**: 1158–1160.
8. Gautier CA, Kitada T, Shen J. Loss of PINK1 causes mitochondrial functional defects and increased sensitivity to oxidative stress. *Proc Natl Acad Sci USA* 2008; **105**: 11364–11369.
9. Gelmetti V, Ferraris A, Brusa L, Romano F, Lombardi F, Barzaghi C *et al.* Late onset sporadic Parkinson's disease caused by PINK1 mutations: clinical and functional study. *Mov Disord* 2008; **23**: 881–885.
10. Wood-Kaczmar A, Gandhi S, Yao Z, Abramov AY, Miljan EA, Keen G *et al.* PINK1 is necessary for long term survival and mitochondrial function in human dopaminergic neurons. *PLoS One* 2008; **3**: e2455.
11. Gandhi S, Wood-Kaczmar A, Yao Z, Plun-Favreau H, Deas E, Klupsch K *et al.* PINK1-associated Parkinson's disease is caused by neuronal vulnerability to calcium-induced cell death. *Mol Cell* 2009; **33**: 627–638.
12. Marongiu R, Spencer B, Crews L, Adame A, Patrick C, Trejo M *et al.* Mutant Pink1 induces mitochondrial dysfunction in a neuronal cell model of Parkinson's disease by disturbing calcium flux. *J Neurochem* 2009; **108**: 1561–1574.
13. Plun-Favreau H, Klupsch K, Moisoi N, Gandhi S, Kjaer S, Frith D *et al.* The mitochondrial protease HtrA2 is regulated by Parkinson's disease-associated kinase PINK1. *Nat Cell Biol* 2007; **9**: 1243–1252.
14. Pridgeon JW, Olzmann JA, Chin LS, Li L. PINK1 protects against oxidative stress by phosphorylating mitochondrial chaperone TRAP1. *PLoS Biol* 2007; **5**: e172.
15. Chu CT. A pivotal role for PINK1 and autophagy in mitochondrial quality control: implications for Parkinson disease. *Hum Mol Genet* 2010; **19**: R28–R37.
16. Vives-Bauza C, Zhou C, Huang Y, Cui M, de Vries RL, Kim J *et al.* PINK1-dependent recruitment of Parkin to mitochondria in mitophagy. *Proc Natl Acad Sci USA* 2010; **107**: 378–383.
17. Geisler S, Holmstrom KM, Skujat D, Fiesel FC, Rothfuss OC, Kahle PJ *et al.* PINK1/Parkin-mediated mitophagy is dependent on VDAC1 and p62/SQSTM1. *Nat Cell Biol* 2010; **12**: 119–131.
18. Narendra DP, Jin SM, Tanaka A, Suen DF, Gautier CA, Shen J *et al.* PINK1 is selectively stabilized on impaired mitochondria to activate Parkin. *PLoS Biol* 2010; **8**: e1000298.
19. Wang X, Winter D, Ashrafi G, Schlehe J, Wong YL, Selkoe D *et al.* PINK1 and Parkin target Miro for phosphorylation and degradation to arrest mitochondrial motility. *Cell* 2011; **147**: 893–906.
20. Michiorri S, Gelmetti V, Giarda E, Lombardi F, Romano F, Marongiu R *et al.* The Parkinson-associated protein PINK1 interacts with Beclin1 and promotes autophagy. *Cell Death Differ* 2010; **17**: 962–974.
21. He C, Levine B. The Beclin 1 interactome. *Curr Opin Cell Biol* 2010; **22**: 140–149.
22. Zhou F, Yang Y, Bcl-2 XingD. and Bcl-xL play important roles in the crosstalk between autophagy and apoptosis. *FEBS J* 2011; **278**: 403–413.
23. Krajewska M, Mai JK, Zapata JM, Ashwell KW, Schendel SL, Reed JC *et al.* Dynamics of expression of apoptosis-regulatory proteins Bid, Bcl-2, Bcl-X, Bax and Bak during development of murine nervous system. *Cell Death Differ* 2002; **9**: 145–157.
24. Greene AW, Grenier K, Aguileta MA, Muise S, Farazifard R, Haque ME *et al.* Mitochondrial processing peptidase regulates PINK1 processing, import and Parkin recruitment. *EMBO Rep* 2012; **13**: 378–385.
25. Maiuri MC, Le Toumelin G, Criollo A, Rain JC, Gautier F, Juin P *et al.* Functional and physical interaction between Bcl-X(L) and a BH3-like domain in Beclin-1. *EMBO J* 2007; **26**: 2527–2539.
26. Poruchynsky MS, Wang EE, Rudin CM, Blagosklonny MV, Fojo T. Bcl-xL is phosphorylated in malignant cells following microtubule disruption. *Cancer Res* 1998; **58**: 3331–3338.
27. Clem RJ, Cheng EH, Karp CL, Kirsch DG, Ueno K, Takahashi A *et al.* Modulation of cell death by Bcl-XL through caspase interaction. *Proc Natl Acad Sci USA* 1998; **95**: 554–559.
28. Juenemann K, Reits EA. Alternative macroautophagic pathways. *Int J Cell Biol* 2012; **2012**: 189794.
29. Upreti M, Galitovskaya EN, Chu R, Tackett AJ, Terrano DT, Granell S *et al.* Identification of the major phosphorylation site in Bcl-xL induced by microtubule inhibitors and analysis of its functional significance. *J Biol Chem* 2008; **283**: 35517–35525.
30. Du L, Lyle CS, Chambers TC. Characterization of vinblastine-induced Bcl-xL and Bcl-2 phosphorylation: evidence for a novel protein kinase and a coordinated phosphorylation/dephosphorylation cycle associated with apoptosis induction. *Oncogene* 2005; **24**: 107–117.
31. Kazi A, Smith DM, Zhong Q, Dou QP. Inhibition of bcl-x(l) phosphorylation by tea polyphenols or epigallocatechin-3-gallate is associated with prostate cancer cell apoptosis. *Mol Pharmacol* 2002; **62**: 765–771.
32. Mellor HR, Rouschop KM, Wigfield SM, Wouters BG, Harris AL. Synchronised phosphorylation of BNIP3, Bcl-2 and Bcl-xL in response to microtubule-active drugs is JNK-independent and requires a mitotic kinase. *Biochem Pharmacol* 2010; **79**: 1562–1572.

33. Levine B, Sinha S, Kroemer G. Bcl-2 family members: dual regulators of apoptosis and autophagy. *Autophagy* 2008; **4**: 600–606.
34. Edlich F, Banerjee S, Suzuki M, Cleland MM, Arnoult D, Wang C *et al.* Bcl-x(L) retrotranslocates Bax from the mitochondria into the cytosol. *Cell* 2011; **145**: 104–116.
35. Shimizu S, Konishi A, Kodama T, Tsujimoto Y. BH4 domain of antiapoptotic Bcl-2 family members closes voltage-dependent anion channel and inhibits apoptotic mitochondrial changes and cell death. *Proc Natl Acad Sci USA* 2000; **97**: 3100–3105.
36. Ofengeim D, Chen YB, Mikawaki T, Li H, Sacchetti S, Flannery RJ *et al.* N-terminally cleaved Bcl-x(L) mediates ischemia-induced neuronal death. *Nat Neurosci* 2012; **15**: 574–580.
37. Tozser J, Bagossi P, Zahuczky G, Specht SI, Majerova E, Copeland TD *et al.* Effect of caspase cleavage-site phosphorylation on proteolysis. *Biochem J* 2003; **372**: 137–143.
38. Inzelberg R, Jankovic J. Are Parkinson disease patients protected from some but not all cancers? *Neurology* 2007; **69**: 1542–1550.
39. Unoki M, Nakamura Y. Growth-suppressive effects of BPOZ and EGR2, two genes involved in the PTEN signaling pathway. *Oncogene* 2001; **20**: 4457–4465.
40. Berthier A, Navarro S, Jimenez-Sainz J, Rogla I, Ripoll F, Cervera J *et al.* PINK1 displays tissue-specific subcellular location and regulates apoptosis and cell growth in breast cancer cells. *Hum Pathol* 2011; **42**: 75–87.
41. Jin Y, Murata H, Sakaguchi M, Kataoka K, Watanabe M, Nasu Y *et al.* Partial sensitization of human bladder cancer cells to a gene-therapeutic. *Oncol Rep* 2012; **27**: 695–699.
42. Chan EY, Longatti A, McKnight NC, Tooze SA, Kinase-inactivated ULK. proteins inhibit autophagy via their conserved C-terminal domains using an Atg13-independent mechanism. *Mol Cell Biol* 2009; **29**: 157–171.
43. Maya R, Oren M. Unmasking of phosphorylation-sensitive epitopes on p53 and Mdm2 by a simple Western-phosphatase procedure. *Oncogene* 2000; **19**: 3213–3215.

Supplementary Information accompanies this paper on Cell Death and Differentiation website (http://www.nature.com/cdd)